Modeling Studies on Adsorption of Pb(Ii) and Hg(Ii) by using *Acalypha Indica*

N.P.Krishnan[1], M. Ilayaraja[2], R. Sayee Kannan[2]*

[1]*Department of Chemistry, K.L.N College of Engineering, Pottapalayam-630611, Tamil Nadu, India.*
[2]*PG & Research, Department of Chemistry, Thiagarajar College,Madurai-625009, Tamil Nadu, India.*

Abstract

The research article describes the experimental and modeling study for the adsorptive removal of Pb (II) and Hg (II) from aqueous matrices using an Acalypha Indica (ACI) as a low cost and eco-friendly adsorbent. The rate of adsorption was investigated under various experimental parameters such as contact time, adsorbent dose, metal ion concentration and temperature. The kinetics, equilibrium and thermodynamic studies were assessed to find out the efficiency of the adsorption process. The equilibrium uptake capacity of the adsorption process was found with Langmuir and Jovanoic adsorption isotherm equations and it was evaluated by dimensionless separation factor (R_L). The dynamics of adsorption was predicted by pseudo-first order, pseudo-second order Lagergren's equation and intra - particle diffusion model. Adsorption feasibility was assessed with thermodynamic parameters such as isosteric heat of adsorption (ΔH∘), standard entropy (ΔS∘) and Gibbs free energy (ΔG∘) using Vant Hoff plot. The adsorbent was characterized with FT-IR, SEM with EDX, BET and XRD.

Keywords - *Acalypha Indica , Adsorption, Mercury ,Modeling, Lead, .*

I. INTRODUCTION

Heavy metal pollution caused by agriculture and manufacturing (e.g., mining and automobile manufacturing) industries is a worldwide problem [1]. The pollutants can contaminate rivers and lakes, and are a major threat to public safety, especially for drinking water. For example, according to the World Health Organization (WHO), the health effects of long term exposure upto 0.015 ppm of Pb(II) caused headache, irritability, abdominal pain and various symptoms related to the nervous system [2], and long-term exposure to Cr(VI) levels over 0.1 ppm which can cause respiratory problems, kidney and liver damage [3].

For heavy metal removal, the adsorption method is a cost-effective approach [4-7], which also offers great flexibility in design and operations. In some instances, adsorption can be used together with filtration to yield better efficiency in applications such as potable water purification. As most sorption processes are reversible, adsorbents can be regenerated by a suitable desorption process. These adsorbents include activated carbon, carbon nano tubes [8] and bio-adsorbents (e.g., shrimp and crab shells, dead bacteria, spent yeast) [9,10]. The application of such adsorbents often requires post-treatment after adsorption. Sometimes the complete separation and removal of adsorbents from water can be difficult and can cause additional environmental problems [11-13]. Heavy metal removal by membrane filtration has also been well-demonstrated in the industry. Typically, membrane filtration approaches are not as cost-effective as adsorption because the processes often involve nanofiltration or reverse osmosis, which invariably have high energy costs and can require high pressure [14-18].

In the present study, *Acalypha Indica* used as a low cost adsorbent for the removal of Pb (II) and Hg (II) metal ions from aqueous solution. The effects of different parameters including initial concentration of metal ion solution and contact time, adsorbent dose and temperature were investigated. The adsorption kinetics, isotherms and thermodynamic properties were also explored.

II. MATERIALS AND METHODS

A. Materials

The Mercury chloride ($HgCl_2$, M.W. 271.50) and Lead nitrate $Pb(NO_3)_2$, M.W. 331.21) was obtained from RANKEM chemicals, New Delhi, India. All the chemicals used are analytical grade. The double distilled water was used throughout the investigation.

B. Adsorbent

The Acalypha *Indica* was collected from Thirupparankundram in Madurai district, Tamil Nadu, India. The material was first washed several times with tap water to remove various impurities. Afterwards, it was washed several times with distilled water. The material was pulvarized into small pieces and kept at room temperature. The material was crushed and ground into a fine powder. The obtained powder was dried at 110˚C for 24 h and kept in an air tightened

bottle. So that it could be further used to adsorption studies and characterization.

C. Adsorption Experiments

Batch mode adsorption studies were carried out by adding certain amount of adsorbent and 40 ml of metal ion solutions of certain concentrations, Dose, contact time and Temperatures in a thermo stated water bath shaker with a shaking of 200 rpm. The samples were withdrawn from the shaker at predetermined time intervals and solutions were separated from the adsorbent by centrifugations at 4000 rpm for 5 min. To determine the residual metal ion concentration, the absorbance of the supernatant solution was measured before and after treatment. Concentration was measured using atomic absorption (Elico SL-173) spectrometry at the wavelength of 283.3 253.7 nm for Pb (II) and Hg (II) respectively. Experiments were carried out twice and the concentrations given were average values. The initial metal ion concentrations in the test solution and the contact time were varied to investigate their effect on the adsorption kinetics. The pH of the metal ion solution was adjusted by using NaOH or HCl solution by pH meter. The adsorption studies were carried out at different temperatures (308K, 313K and 318K). This is used to determine the effect of temperature on the thermodynamic parameters.

The amount of adsorption in batch experiments, q (mg g^{-1}) (1) and adsorption efficiency (2) were calculated as follows:

$$q = (C_o - C_e) V / m \quad (1)$$

$$\text{Efficiency (\%)} = (C_o - C_e) / C_o \times 100 \quad (2)$$

Where C_o is the initial concentration (mg.L^{-1})

C_e is the equilibrium concentration (mg.L^{-1})

V is the volume of solution (mL)

M is the mass of adsorbent (g)

q is the amount of adsorbed (mg/g)

D. Surface Characteristic of the Adsorbent

Surface area and porous size distribution of *Acalypha Indica* sample were measured by nitrogen adsorption analysis (Quantachrome V5.02). Crystal structure of sample was determined by performing X-ray diffraction (XRD) on SHIMADZU 6000 X-ray diffraction spectrometer. Surface morphologies were examined by a scanning electron microscope (SEM, JEOL (JSM 6390) with the working distance of 9.9 mm and an accelerating voltage of 30 keV. The SEM was equipped with an energy dispersion spectrometer (EDX) and it was used to perform the analysis of chemical constituents of the adsorbent. Infrared absorption spectroscopy (IR) spectra were measured at

room temperature on a Fourier transform infrared (FT-IR) spectroscopy (8400s SHIMADZU spectrometer) using the KBr pellet technique.

3. Results and Discussion

3.1. Characterization of the adsorbent

BET:

The surface area of ACI was found to be 51.93 m^2/g. Total pore volume is 5.2 cm^3/g and pore size is 747.9Å. ACI has a relatively high promising surface area than previously reported adsorbents.
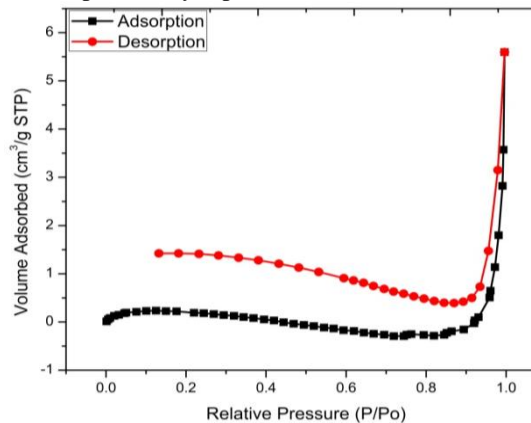
Fig. 1. Adsorption-Desorption Isotherms of Nitrogen at 77 K on ACI

FT-IR:

The functional groups of samples were confirmed by FT-IR and the results are shown in Fig. 2. The samples contained ACI, ACI-Hg (II) and ACI-Pb (II).

As shown in Fig. 2a, in the spectrum of ACI the absorption peak at 3288.2 is assigned to the -OH stretching vibration. FT-IR data of ACI showed that characteristic band at 2913.6, 1729.2, 1418.6 and 1026.1 cm^{-1} correspond to the C-CH$_3$,C=O,C-H bending vibration and C-O-C stretching vibrations respectively.

The FT-IR spectrum of Hg(II) metal ions adsorbed onto ACI was exhibited in Fig.2b. After adsorption the intensity of free -OH group was increased from 3288.2 to 3328.6 cm^{-1}. The new band that appeared at 1630.8 cm^{-1} was assigned to C=C non-conjugated stretching vibration. The C-CH$_3$, C=O, C-H bending vibration and C-O-C stretching vibrations intensity was slightly increased more than ACI. These findings suggest that there is attachment of Hg (II) metal ions on the ACI.

Fig. 2c indicated that mostly the bonded C=O stretching, C=C bending vibrations, C-O-C vibrations and C-H bending vibrations were involved in Pb (II) metal ion adsorption. There were clear band shifts and

intensity decrease in Fig. 2c. These findings suggest that there is attachment of Pb (II) metal ions on ACI.
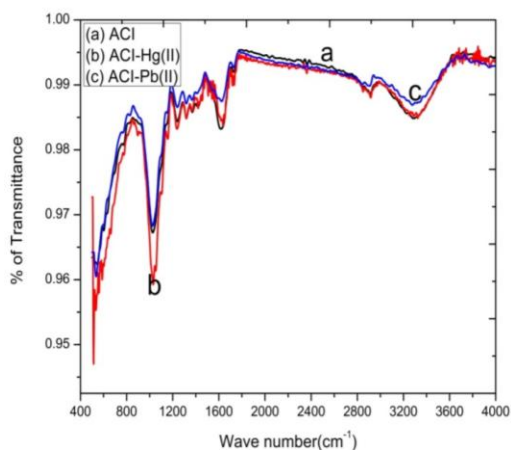
Fig. 2. FTIR Spectra of (a) ACI (b) ACI-Hg (II) (c) ACI-Pb (II)

XRD:

The XRD patterns as shown in Fig.3 were performed to analyze the crystalline nature. The characteristic 20˚-30˚ peaks of ACI were discernible in raw material, the diffraction spectrum of ACI did not show any obvious crystalline peak at the scan range 10-90˚ thereby indicating the amorphous phase of ACI.
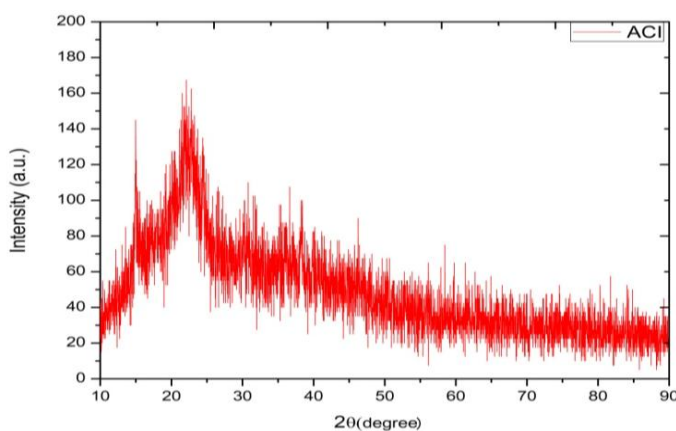
Fig. 3. XRD Pattern of ACI

SEM:

The morphologies of as-prepared adsorbent were further investigated by scanning electron microscopy (SEM), as shown in Fig 4.
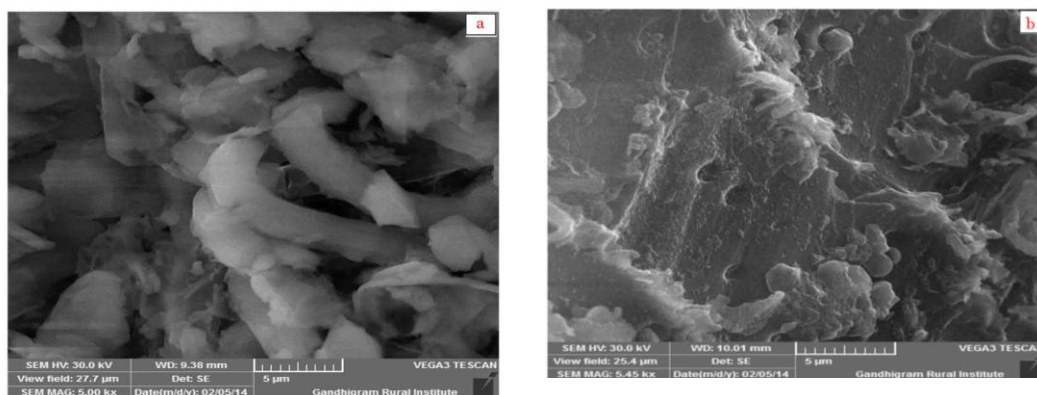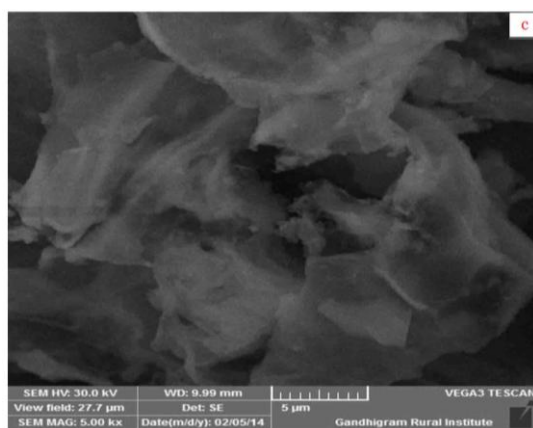
Fig. 4. The SEM Images of (a) ACI (b) ACI-Hg (II) (c) ACI-Pb (II)

The original ACI particles (Fig. 4 a) show as dispersed and smooth. Clearly the particle fragments and irregular structure on the surface are beneficial for the metal ions to diffuse to the inner adsorption sites located in the interior portion of the adsorbent. Fig.4b and Fig.4c show micro graphs of the ACI surface after adsorbed Hg (II) and Pb (II) ions. These are covered with some small particulates on the surface suggesting that Hg (II) and Pb (II) ions have been adsorbed.

EDX:

Further confirmation of the adsorption of Hg (II) and Pb (II) on ACI was done by energy dispersive X-ray analysis (EDX). Fig.5a for the unloaded ACI did not show any characteristic signal for metal ions, but only showed for the four major constituents, i.e., C, O, Mg, P, Cl, K, Ca and S. For Hg(II) and Pb(II) loaded ACI (Fig.5b and 5c) signals of presence of Hg(II) and Pb(II) were observed. This showed the diffusion or accumulation of metal ions onto the surface of ACI.
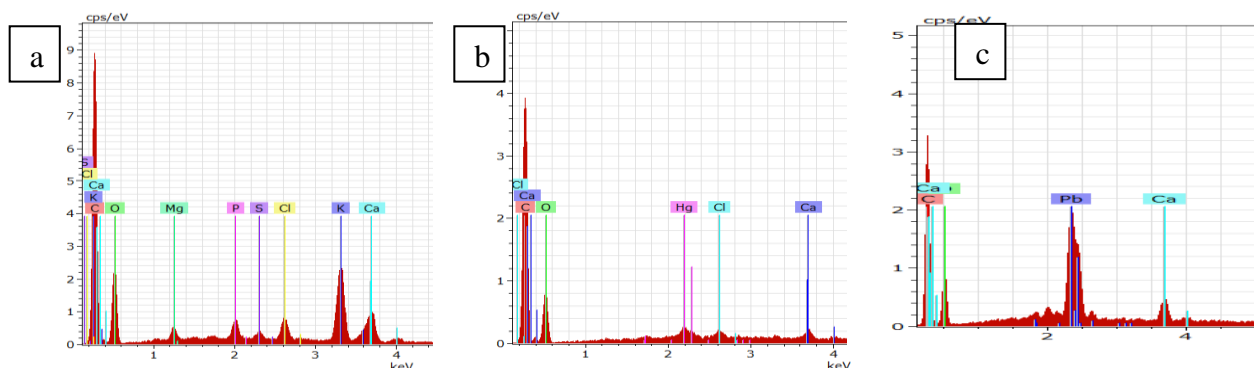
Fig. 5. Energy Dispersive Spectra of (a) ACI (b) ACI-Hg (II) (c) ACI-Pb (II)

3.2. Effect of initial concentrations

The effect of initial lead and mercury ion concentration was studied at different initial metal ion concentrations in the range between 10-50 mg/L at 298K with 0.250g ACI at 240 min. The percentage of lead and mercury ions adsorption at different metal ion concentrations using ACI, decreased with increase in metal ion concentration. This may be due to saturation of active adsorption sites onto ACI. The effect of initial concentration on the removal of Pb(II) and Hg(II) by the adsorbent is indicated in Table 1.

Table.1. Effect of Initial Concentrations of Hg (II) and Pb (II)

Concentrations (ppm)	Adsorption efficiency (%)					Amount of adsorbed, q (mg/g)				
	10	20	30	40	50	10	20	30	40	50
Hg (II)	86.5	29.1	19.0	23.5	25.6	49.4	9.9	5.9	8.0	4.8
Pb (II)	90.8	86.3	80.9	64.9	56.8	55.3	53.6	48.8	36.4	31.3

3.3. Effect of contact time

The effect of contact time on the adsorption of Pb(II) and Hg(II) was at 10 mg/L. The lead and mercury ion adsorption increased with increasing the contact time, the maximum removal of both lead and mercury occurred at 240 min, after which there were no significant changes. The equilibrium was reached at 240 min for the both metal ions. Following this, the adsorption rate was uniform as there was no significant change in adsorption with the increasing time. The initial fast adsorption is due to the availability of more active sites and more functional groups which participate in the lead and mercury uptake till equilibrium is attained and thereafter, there was no further adsorption. All the results are presented in Table 2.

Table.2. Effect of Contact Time

Contact time (min)	Adsorption efficiency (%)						Amount of adsorbed, q (mg/g)					
	30	60	120	180	240	300	30	60	120	180	240	300
Hg (II)	51.4	55.6	64.6	73.4	87.0	87.0	29.1	31.5	36.6	41.6	49.2	49.2
Pb (II)	28.8	40.1	54.0	62.2	92.3	92.3	17.6	24.4	32.9	37.9	56.3	56.3

3.4. Effect of adsorbent mass

The effect of adsorbent dosage on lead and mercury removal was studied by varying the amount ACI between 0.050-0.300g. It is evident from Table 3 that the removal of lead and mercury was increased with increase in ACI dose until a constant value was achieved. That is, the percentage removal, increased from 6.8% to 90.0% for lead and mercury, was increased from 17.1% to 87.9 % as the ACI adsorbent. This can be associated with higher available surface area and more available sorption sites at higher sorbent doses. The optimum adsorbent dosage was found to be lead and mercury for 0.250g of ACI. The adsorption efficiency of both lead and mercury was observed at 90.0% and 87.9% respectively.

Table.3. Effect of Adsorbent Dose

Dose (g)	Adsorption efficiency (%)						Amount of adsorbed, q (mg/g)					
	0.050	0.100	0.150	0.200	0.250	0.300	0.050	0.100	0.150	0.200	0.250	0.300
Hg (II)	17.1	29.5	32.0	58.7	87.9	87.9	48.0	41.2	29.8	41.0	49.1	40.9
Pb (II)	6.8	33.8	53.2	75.5	90.0	90.0	20.8	51.6	54.1	57.6	54.8	45.7

4. MODELING STUDIES

Adsorption isotherm was usually applied to describe the interaction between the adsorbate and the adsorbent. The correlation of equilibrium data is essential for practical design and operation of adsorption systems. In the current study, a comparison of Langmuir, Freundlich, Temkin, D-R and Jovanoic isotherm models was fitted to analyze the equilibrium data.

We used the Langmuir adsorption model to calculate the adsorption capacity [19]. The adsorption isotherms for both Pb (II) and Hg (II) ions were evaluated using the following equation,

$$\frac{C_e}{q_e} = \frac{1}{K_L \times q_m} + \frac{C_e}{q_m} \qquad (3)$$

Where, q_e is the amount of metal ions adsorbed, q_m is the maximum adsorption capacity and K_L is the Langmuir bonding energy coefficient. The K_L and q_m can be calculated from the intercept and slope of the linear plot of C_e/q_e against C_e shown in Fig.6.
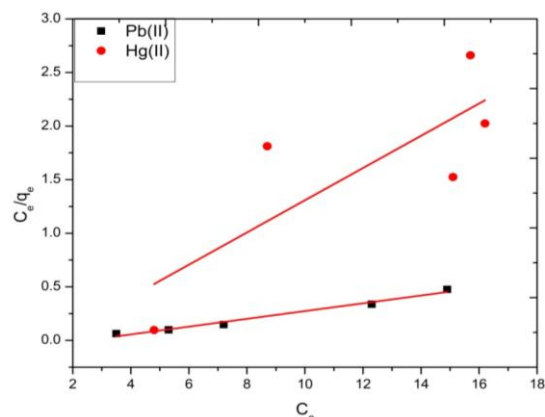
Fig. 6. Langmuir isotherm plots for the adsorption of Pb (II) and Hg (II) onto ACI

It is obvious that, the Langmuir adsorption isotherm is more suitable to describe the adsorption equilibrium ($R^2 > 0.981$). Therefore, monolayer coverage of Pb (II) on ACI particles is assumed with the maximum adsorption capacity of 40.46 mg/g.

According to [20], the essential characteristics of Langmuir isotherm can be explained in terms of dimensionless constant separation factor (R_L), which is defined by the following equation:

$$R_L = 1/1 + K_L C_o \qquad (4)$$

In this equation, K_L (L/mg) is the Langmuir constant related to the energy of adsorption and C_o (mg/L) is the initial concentration of both Pb (II) and Hg (II) ions. The R_L value indicates the type of the isotherm to be either unfavorable ($R_L>1$), linear ($R_L=1$), favorable ($0<R_L<1$), or irreversible ($R_L=0$). It is clear from Table. 4 that all R_L values lie between 0 and 1 indicating the favorable sorption of Pb(II) and Hg(II) ions by the ACI.

Table.4. Separation factor

Concentration	Hg (II) (ppm)					Pb (II) (ppm)				
	10	20	30	40	50	10	20	30	40	50
R_L	0.036	0.060	0.066	0.061	0.110	0.064	0.063	0.065	0.074	0.07

The Freundlich isotherm is expressed by an empirical equation, which is represented by [21]

$$\log q_e = \log K_F + \ 1/n \ \log C_e \qquad (5)$$

where,' K_F' and 'n' are the Freundlich isotherm constants indicating the adsorption capacity and adsorption intensity, respectively. The values of K_F and n can be obtained from the plot of $\log q_e$ against $\log C_e$. The value of n >1 indicates (2.475 and 0.783) favorable and heterogeneous adsorption of Pb (II) and Hg (II) onto ACI. Both the metals did not follow the Freundlich isotherm as closely as the Langmuir isotherm.

The Dubinin–Radushkevich [22] isotherm has been used to describe the sorption of metal ions; the equation has the form:

$$\ln q_e = \ln q_m - \beta \varepsilon^2 \qquad (6)$$

where, q_e is the amount of Pb(II) and Hg(II) adsorbed per unit weight of adsorbent (mg/g), q_m is the maximum sorption capacity, β is the activity coefficient related to mean sorption energy, and ε is the Polanyi potential, which is equal to:

$$\varepsilon = RT \ln (1+1/C_e) \qquad (7)$$

where, R is the gas constant (kJ/mol K) and T is the temperature (K).The saturation limit q_m may represent the total specific microspore volume of the sorbent. The sorption potential is independent of the temperature but varies according to the nature of sorbent and sorbate.

The biosorption type based on the D-R model can be predicted by the mean free energy (kJ/mol) employing Eq.8 [23]

$$\mathbf{E = 1/ (2\beta)^{1/2}} \qquad (8)$$

The magnitude of E may characterize the type of the adsorption as chemical ion exchange (E=8-16 kJ/mol), or physical adsorption (E<8 kJ/mol). The mean free energy of adsorption for the present study was found to be 0.499 kJ/mol for Pb (II) and 2.2 kJ/mol for Hg (II). This implies that, the adsorption of Pb (II) on ACI may

be considered as physical adsorption process, and the Hg (II) as chemical adsorption process.

Temkin isotherm models assume that the fall in the heat of sorption is linear rather than logarithmic. The data were analyzed according to the linear form of the Temkin model [24].

$$q_e = B_1 \ln K_T + B_1 \ln C_e$$
(9)

The isotherm constants B_1 and K_T are related to the maximum binding energy and heat of adsorption. The B_1 and K_T can be calculated from the intercept and slope of the linear plot of q_e against $\ln C_e$.

The Jovanoic isotherm [25], which is based on the same assumptions of the Langmuir isotherm, also considers the possibility of some mechanical contacts between the adsorbing and desorbing molecules on the homogeneous surface and can be represented in a linear form as follows:

$$\ln q_e = \ln q_m + K_J C_e$$
(10)

where, q_m is the maximum amount adsorbed (in mg/g) and K_J (in L/mg) is the constant related to the energy of adsorption. The q_m and K_J can be calculated from the intercept and slope of the linear plot of $\ln q_e$ against C_e (Fig.7).
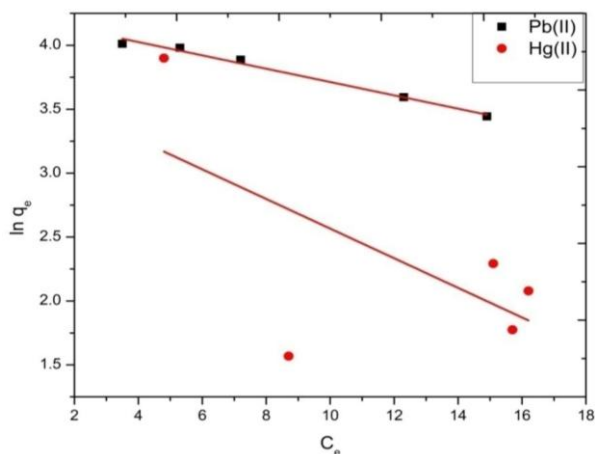
Fig. 7. Jovanoic isotherm plots for the adsorption of Pb (II) and Hg (II) onto ACI

As seen from Table 5, the correlation coefficients showed that the Langmuir and Jovanoic model was the best fitted in five isotherm models. Freundlich, Temkin and Dubinin–Radushkevich models were not very good. The Langmuir isotherms were best fit model for the adsorption of Pb (II); the maximum adsorption capacity of Pb (II) was 27.77 mg/g. The Jovanoic isotherm model well described in Pb (II) onto ACI. The maximum amount adsorbed was 4.23 and 3.72 mg/g for Pb (II) and Hg(II) respectively.

Table.5. Different adsorption isotherm model parameters for the adsorption of Pb (II) and Hg (II) on ACI

Mathematical models	Parameters	Pb(II)	Hg(II)
Langmuir isotherm	R^2	0.981	0.648
	K_L	40.46	76.93
	q_m (mg/g)	27.77	6.666
Freundlich isotherm	R^2	0.916	0.534
	$K_F \times 10^{-2}$	399.9	242.1
	n	2.475	0.783
Temkin isotherm	R^2	0.939	0.702
	B_1	17.37	30.09
	K_T	80.19	87.74
D-R isotherm	R^2	0.672	0.892
	β	2.006	0.001
	q_m (mg/g)	179.47	319.88
	E kJ/mol	0.499	2.2×10^{-5}
Jovanoic isotherm	R^2	0.987	0.407
	K_J (L/mg)	0.052	0.115
	q_m (mg/g)	4.23	3.72

5. KINETIC STUDIES

A study of adsorption kinetics is expected as it can provide information on the mechanism of adsorption. The pseudo-first -order, pseudo-second-order and intraparticle diffusion models were employed to investigate the kinetics of adsorption of Pb(II) and Hg(II) on ACI.

5.1 Pseudo-first-order model

The pseudo-first-order kinetic model is expressed by the following equation [26, 27]:

$$\ln (q_e-q_t) = \ln q_e - k_1 t \qquad (11)$$

where, q_e (mg/g) and q_t (mg/g) are the adsorption capacity at equilibrium and time t (min), respectively; k_1 (min^{-1}) is the rate constant of pseudo-first-order kinetic model. Values of k_1 and q_e can be obtained from the slope and intercept of the plot ln (q_e-q_t) versus t. The values of correlation coefficient (R^2) are relatively low. This indicated that the adsorption process did not fit the pseudo-first-order model.

5.2 Pseudo-second-order model

The pseudo-second-order model is expressed as [28]:

$$\frac{t}{q_t} = \frac{1}{k_2 q^2_e} + \frac{t}{q_e} \qquad (12)$$

where, k_2 (g/mg/min) is the second-order rate constant of adsorption. The plot of t/q_t versus t shows a linear relationship. Values of k_2 and equilibrium adsorption capacity q_e were calculated from the intercept and slope of the plot shown in Fig.8. The R^2 values of Hg (II) & Pb(II) is 0.980 & 0.878 respectively.
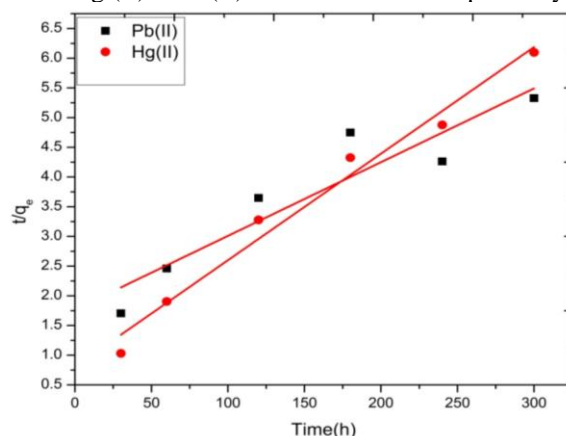
Fig. 8. Pseudo-second-order kinetic plots for adsorption of Pb (II) and Hg (II) onto ACI

5.3 Intra-particle diffusion model

The intraparticle diffusion model [29] was used to identify the diffusion mechanism during adsorption process. It is described using the following equation:

$$q_t = k_{id}t^{0.5} + C \qquad (13)$$

where, k_{id} (mg g^{-1}min$^{-0.5}$) is the rate constant of the intra-particle diffusion model and C (mg/ g) reflects the boundary layer effect. The k_{id} and C can be determined from the slope and intercept of the linear plot of q_t against $t^{0.5}$.

The pseudo-first-order, pseudo-second-order and intra-particle diffusion models were used to understand the kinetic nature of Pb (II) and Hg (II) onto ACI adsorption system. All the values were presented in Table.6. All the experimental data showed better agreement with pseudo-second-order model in terms of higher correlation coefficient value ($R^2 > 1$), which suggested that the adsorption rate of Hg(II) onto ACI might be controlled by chemisorptions mechanism. The rate controlling step consisted of valence forces through sharing or exchange of electrons between the adsorbent surface and adsorbate ions without any involvement of mass transfer in solution. The value of pseudo-second-order rate constant, k_2, was 6.787 g/mg/min for Pb (II) was and 0.021 g/mg/min for Hg (II).

Table.6. Kinetic Parameters for the Adsorption of Pb (II) and Hg (II) on ACI

Mathematical models	Parameters	Pb(II)	Hg(II)
First-order kinetics	R^2	0.874	0.697
	k_1 (min^{-1})	0.010	0.016
	q_e (mg/g)	635.3	26.66
Second-order kinetics	R^2	0.878	0.980
	k_2 g/mg/min	6.787×10^{-3}	0.021
	q_e (mg/g)	83.33	58.82
Intra-particle diffusion	R^2	0.945	0.965
	k_{id} g/mg/min$^{1/2}$	3.435	1.862
	C (mg/g)	17.67	2.747

6. EFFECT OF TEMPERATURE AND THERMODYNAMIC DATA

The adsorption tests were performed by batch technique in single system at 308K, 318K, and 328K, respectively. For kinetic studies, a series of 250ml flask were used and each flask was filled with ACI at mass loadings 0.250g for both Pb (II) and Hg (II) solution at 10ppm metal solutions. The percentage removal of Pb (II) and Hg (II) are presented in Table 7.

Table.7. Effect of Temperature

Metal ions	Adsorption Efficiency (%)			Amount of adsorbed, q (mg/g)		
	308K	318K	328K	308K	318K	328K
Hg (II)	56.3	66.9	87.6	32.1×10^2	38.2×10^2	50.0×10^2
Pb (II)	32.8	61.1	89.2	20.0×10^2	37.2×10^2	54.4×10^2

The adsorption experiments at different temperatures were also performed to evaluate the influence of temperature (308–328 K). The thermodynamic property of the adsorbent-metal (ACI –metal ions) system was calculated using the following equation [30]:

$$K_L = \frac{q_e}{C_e} \qquad (14)$$

where, K_L is the Langmuir constants; C_e is the concentration of solute adsorbed on the resin at equilibrium, mg/ L.

$$\Delta G° = -RT \ln K_L \qquad (15)$$

The change in enthalpy ($\Delta H°$) and entropy ($\Delta S°$) was determined from the slope and intercept of van't Hoff plot of ln K_L versus 1/T plot (Fig.9), according to the following equation:

$$\ln K_L = \frac{\Delta S°}{R} - \frac{\Delta H°}{RT} \qquad (16)$$
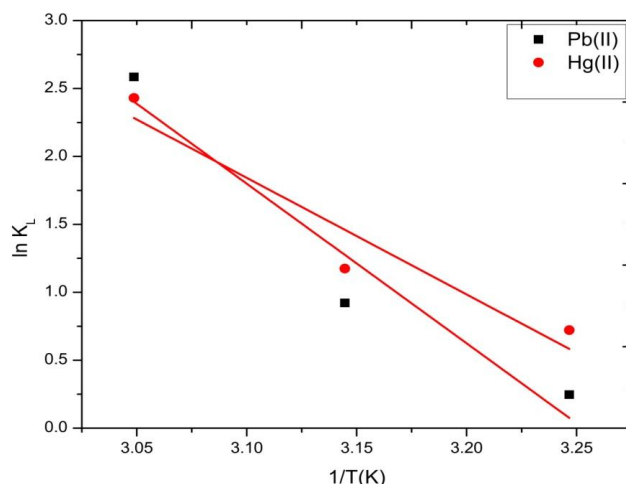
Fig. 9. van't Hoff plots of ln K_L versus 1/T for the adsorption of Pb(II) and Hg(II) onto ACI

where, R is the gas constant (8.314 J/mol K), T is the temperature (in K). The correlation coefficient for the linear plot for Pb (II) and Hg (II) was $R^2 = 0.935$ and $R^2 = 0.922$ respectively. Values of the standard Gibbs free energy change for the adsorption process obtained from Eq. (15) were listed in Table 8.

The values of $\Delta S°$, $\Delta H°$ and $\Delta G°$ were computed from the slope and intercept of plot between ln K_L versus 1/T, as shown in Fig. 9. The calculated values of $\Delta S°$, $\Delta H°$ and $\Delta G°$ are shown in Table 8. The

positive value of isosteric heat of adsorption ($\Delta H°$) reveals that the adsorption process is endothermic in nature and the competition between the solute and the solvent particle involves a complex phenomenon on the solid surface. Moreover the process of adsorption and desorption takes place simultaneously. The experimental value of the Gibbs free energy ($\Delta G°$) shows a negative sign intimating that the process is spontaneous in nature. The positive value of the ($\Delta S°$) implies that the increment of an orderliness between the adsorbate and the adsorbent molecules.

Table.8. Thermodynamic Parameters for the Adsorption of Pb(II) and Hg(II) on ACI

Metal ions	Thermodynamics parameters					
	R^2	$\Delta H°$ J/mol	$\Delta S°$ J/mol K	$-\Delta G°$(kJ/mol)		
				308K	318K	328K
Hg(II)	0.922	71.37	236.1	1847.5	3105.6	6627.4
Pb(II)	0.935	97.68	317.8	632.7	2436.5	7049.8

7. CONCLUSION

From the studies it may concluded that *Acalypha Indica* is eco-friendly and a cheap material that could be used as a potential adsorbent for the removal of Pb(II) and Hg(II) metal ions from aqueous solution. Based on these results, the optimum contact time is considered to be 240 min and adsorbent dosage as 0.250 g. In the current study, Langmuir, Freundlich, Temkin, D-R and Jovanoic isotherm models were compared and fitted to analyze the equilibrium data. The experimental result shows that the Langmuir and Jovanoic isotherm was the best suited model when compared to other isotherm models. The result of dimensionless separation factor implies that the adsorption process was favorable and the value of

R_L lies between 0 to 1. The kinetic data tends to fit very well in the pseudo-second-order kinetics model, indicating that the chemisorption of the heavy metal ions occur on the natural adsorbent. The negative value of $\Delta G°$ shows that the process was spontaneous in nature and progression of more negative value indicates that equilibrium increases with temperature. The positive value of ($\Delta H°$) reveals that the adsorption process is endothermic in nature and the competition between the solute and the solvent particle involves a complex phenomenon on the solid surface. Moreover the process of adsorption and desorption takes place simultaneously. The positive value of the ($\Delta S°$) implies an increment of orderliness between the adsorbate and the adsorbent molecules. The FT-IR spectrum shows a

good reduction in peak height and peak shifting before and after adsorption of Pb(II) and Hg(II) metal ions.SEM images shows well-defined and characterized morphological images that are evident for the strong adsorption of the metals on the surface of the natural adsorbents.

REFERENCE

[1] O Weber, RW Scholz, R Buhlmann, D Grasmuck. Risk perception of heavy metal soil contamination and attitudes toward decontamination strategies. Risk Anal 21(5):2001; 967-77.

[2] L Jarup. Hazards of heavymetal contamination. BrMed Bull 68(1):2003;167-82.

[3] RA Morello-Frosch,TJ Woodruff,DA Axelrad,JC Caldwell.Air toxics and health risks in California:the public health implications of outdoor concentrations.RiskAnal 20(2):2000;273-91.

[4] XW Peng, LX Zhong, JL Ren, RC Sun. Highly effective adsorption of heavy metal ions from aqueous solutions by macroporous xylan-rich hemicelluloses-based hydrogel. J Agric Food Chem 60(15):2012; 3909-16.

[5] Y Pang, GM Zeng, L Tang, Y Zhang, YY Liu, XX Lei. PEI-grafted magnetic porous powder for highly effective adsorption of heavy metal ions. Desalination 281:2011; 278-84.

[6] YL Zhao, QA Gao, T Tang, Y Xu, D Wu. Effective NH_2-grafting on mesoporous SBA-15 surface for adsorption of heavy metal ions. Mater Lett 65(6):2011; 1045-7.

[7] IL Lagadic, MK Mitchell, BD Payne. Highly effective adsorption of heavy metal ions by a thiol-functionalized magnesium phyllosilicate clay. Environ Sci Technol 35(5):2001; 984-90.

[8] MA Salam, G Al-Zhrani, SA Kosa. Simultaneous removal of copper(II), lead(II), zinc(II) and cadmium(II) from aqueous solutions by multi-walled carbon nanotubes. Comptes Rendus Chim 15(5):2012; 398-408.

[9] M Thirumavalavan, YL Lai, LC Lin, JF Lee. Cellulose-based native and surface modified fruit peels for the adsorption of heavy metal ions from aqueous solution: Langmuir adsorption isotherms. J Chem Eng Data 55(3):2010; 1186-92.

[10] YF Zhou, RJ Haynes. A comparison of organic wastes as bio-adsorbents of heavy metal cations in aqueous solution and their capacity for desorption and regeneration. Environ Earth Sci 66(4):2012; 1137-48.

[11] Z Reddad, C Gerente, Y Andres, P Le Cloirec. Adsorption of several metal ions onto a low-cost biosorbent: Kinetic and equilibrium studies. Environ Sci Technol 36(9):2002; 2067-73.

[12] D Kratochvil, P Pimentel, B Volesky. Removal of trivalent and hexavalent chromium by seaweed biosorbent. Environ Sci Technol 32(18):1998; 2693-8.

[13] GY Yan, T Viraraghavan. Heavy-metal removal from aqueous solution by fungus Mucor rouxii. Water Res 37(18):2003; 4486-96.

[14] P Religa, A Kowalik, P Gierycz. Effect of membrane properties on chromium (III) recirculation from concentrate salt mixture solution by nanofiltration.Desalination274(1-3): 2011; 164-70.

[15] M Muthukrishnan, BK Guha. Effect of pH on rejection of hexavalent chromium by nanofiltration. Desalination 219(1-3):2008; 171-8.

[16] MT Ahmed, S Taha, T Chaabane, D Akretche, R Maachi, Dorange G. Nanofiltration process applied to the tannery solutions. Desalination 200(1-3):2006; 419-20.

[17] M Taleb-Ahmed, S Taha, R Maachi, G Dorange. The influence of physicochemistry on the retention of chromium ions during nanofiltration. Desalination 145(1-3):2002; 103-8.

[18] A Hafiane, D Lemordant, M Dhahbi. Removal of hexavalent chromium by nanofiltration. Desalination 130(3):2000; 305-12.

[19] SY Chen, Y Zou, ZY Yan, W Shen, SK Shi, X Zhang, et al. Carboxymethylatedbacterialcellulose for copper and lead ion removal. J Hazard Mater 161(2-3):2009; 1355-9.

[20] K.R. Hall, L.C. Eagleton, A. Acrivos & T. Vermevlen, Ind. Eng. Chem. Fund. 5:1966; 212-219.

[21] H.M.F. Freundlich, Over the adsorption in solution, J. Phys. Chem. 57:1906; 385–470.

[22] M. M. Dubinin, L.V. Radushkevich, Proc. Acad. Sci, USSR. 55:1947; 331-333.

[23] K.Y. Foo, B.H. Hameed, Chem. Eng. J. 156:2010;2-10.

[24] M.J.Temkin, and V. Pyzhev. Acta. Physiochim URSS. 12:1940; 217-222.

[25] D.S. Jovanoic, Colloid. Polym. Sci. 235:1969; 1203-1214.

[26] F. Wu, R. Tseng, R. Juang, Kinetic modeling of liquid-phase adsorption of reactive dyes and metal ions on chitosan, Water Res. 35:2001;613–618.

[27] Z. Reddad, C. Gerente, Y. Andres, P.L. Cloirec, Adsorption of several metal ions onto a low-cost biosorbent: kinetic and equilibrium studies, Environ. Sci. Technol.36:2002;2067–3073.

[28] Y.S. Ho, G. Mckay, Pseudo-second order model sorption processes, Process Biochem.34 1999; 451–465.

[29] G. Mckay, H.S. Blair, J. Gardner, The adsorption of dyes in chitin. III. Intraparticle diffusion processes, J. Appl. Polym. Sci. 28:1983; 1767–1778.

[30] K. Biswas, S.K. Saha, V.C. Ghosh, Ind. Eng. Chem. Res. 46:2007; 5346 – 5356.